Measurement of Neutron Capture Cross-Sections for ^{164}Dy

Hyun Dock Kim and Dae Won Lee

Pusan National University

30 Changjeon-dong, Keumjeong-ku, Pusan 609-735, Korea

Guin Yun Kim, Young Seok Lee, In Soo Ko, Moo Hyun Cho, and Won Namkung

POSTECH

San 31, Hyojadong Namgu, Pohang 790-784, Korea.

Tae Ik. Ro and Young Ki Min

Donga University

840 Hadan-dong, Saha-gu, Pusan 604-714, Korea

Masayuki Igashira, Satoshi Mizuno, Toshiro Ohsaki, and Sam Yol Lee

Tokyo Institute of Technology

O-okayama, Meguro-ku, Tokyo 152-8550, Japan

Abstract

The neutron capture cross sections of ^{164}Dy were measured in the neutron energy region of 10 to 90 keV using the 3-MV Pelletron accelerator of the Research Laboratory for Nuclear Reactors at the Tokyo Institute of Technology. Pulsed keV neutrons were produced from the ^{7}Li(p,n)^{7}Be reaction by bombarding a lithium target with the 1.5-ns bunched proton beam from the Pelletron accelerator. The incident neutron spectrum on a capture sample was measured by means of a TOF method with a ^{6}Li-glass detector. Capture γ-rays were detected with a large anti-Compton NaI(Tl) spectrometer, employing a TOF method. A pulse-height weighting technique was applied to observed capture γ-ray pulse-height spectra to derive capture yields. The capture cross sections were obtained by using the standard capture cross sections of ^{197}Au. The present results were compared with the previous measurements and the evaluated values of ENDF/B-VI.

1. INTRODUCTION

Capture cross-sections in keV-neutron energy region are important in the design of reactors as well as in the study of the nuclear physics and astrophysics. The published experimental data are poor both in quality and in quantity. One of the reasons is the difficulty of preparing pure enriched isotopes enough to perform keV-neutron capture cross-section measurement. An anti-Compton NaI(Tl) spectrometer (Igashira *et al*. 1994)　developed by the Research Laboratory for Nuclear Reactors at the Tokyo Institute of Technology (Titech) made possible to perform the experiments with a small amount of sample.

We measured the capture cross-sections for a ^{164}Dy, a metal plate of 15-mm in diameter and 0.2-mm in thickness, in the neutron energy region of 10 to 90 keV with the high efficient capture γ-ray spectrometer. Pulsed keV neutrons were produced from the ^{7}Li(p,n)^{7}Be reaction by bombarding a lithium target with the 1.5-ns bunched proton beam from the Pelletron accelerator of the Research Laboratory for Nuclear Reactors at the Titech. This is the first experiment to use a ^{164}Dy metal instead of the dysprosium oxide (Dy$_2$O$_3$). Since dysprosium oxide powder is generally hygroscopic, the effect of the water in the sample on the previous measurements was taken into account in the analysis of experimental data. We compared the present results with the previous measurements (Fawcett *et al*. 1972, Bokhovko *et al*. 1988, Voss *et al.* 1999) and the evaluated values of ENDF/B-VI (Leonard *et al*. 1967).

2. EXPERIMENT

Measurements for the capture cross-sections of ^{164}Dy were performed in the neutron energy region of 10 to 90 keV using the 3.2-MV Pelletron accelerator. A typical experimental arrangement is shown in Fig. 1. The incident neutron spectrum on a capture sample was measured by means of a time-of-flight (TOF) method with a ^{6}Li-glass scintillation detector. The capture sample was mounted at an angle of 0 degree with respect to the proton beam direction. The distance between the neutron source and the sample was 12 cm. The ^{6}Li-glass detector was mounted 30 cm from the neutron source in order to measure the neutron spectrum. The capture γ-rays were detected with a large anti-Compton NaI(Tl) spectrometer which was placed at an angle of 125 degrees with respect to the proton beam direction. The distance between the face of NaI(Tl) spectrometer and the sample is 86.0 cm.

2. 1. Neutron Source

Pulsed keV neutrons were produced by the ^{7}Li(p,n)^{7}Be reaction by bombarding a lithium target mounted at the end of proton beam line. The proton energy was set to 1.903 MeV, which is 22 keV

above the threshold energy of the ^{7}Li(p,n)^{7}Be reaction. At this proton energy, neutrons with energies of 2 to 90 keV are emitted within about 50 degrees with respect to the proton beam direction by kinematics. The pulse repetition rate was 4 MHz and the average proton beam current was about 9 μA. The lithium target was made by evaporating metallic lithium on a copper disk with a diameter of 30 mm and a thickness of 0.4 mm. The diameter of lithium layer was about 20 mm. The lithium target was cooled by water to prevent lithium from being scattered and lost. The temperature of lithium target was kept less than 27 degrees.

2.2. Detector

The incident neutron spectrum on a capture sample was measured by means of a TOF method with a ^{6}Li-glass scintillation detector. A 5.0 mm diameter by 5.0 mm thick ^{6}Li-glass scintillator mounted on the 12.7 mm diameter PM tube was placed at 300 mm from the neutron source and at 2.4 degree with respect to the proton beam direction. The applied HV for the photomultiplier is 1 kV. The detection efficiency was determined by the experiment and Monte-Carlo calculations (Komano 1984, Simizu 1985). The measured time resolution was about 1.8 ns for the γ rays from a ^{60}Co source (Komano 1984, Simizu 1985). A simplified block diagram of electronics for the neutron detector is shown in Fig. 2. The anode output was used as the timing signal for the neutron TOF spectrum, while the dynode output was used as the pulse height signal for the n-γ discrimination. The stop signal for the TOF analysis with a time-to-amplitude converter (TAC) was taken from a time pick-off unit at about 2 m upstream from the neutron target. The TOF spectrum was stored into a personal computer.

The prompt gamma-rays from a neutron capture state to its low-lying states are detected by an anti-Compton NaI(Tl) spectrometer, employing a TOF method. The main detector of spectrometer was a 15.2 cm diameter by 20.3 cm long NaI(Tl) detector, and was centered in a 33.0 cm outer diameter by 35.6 cm long NaI(Tl) hollow Compton-suppression detector. The energy resolution of the main detector was 7.0% (FWHM) at 0.662 MeV, and the time resolution was 4.0 ns (FWHM) for the 0.511 MeV γ rays. The spectrometer was set in a heavy shield consisting of borated paraffin, borated polyethylene, cadmium, and potassium free lead (Igashira *et al.* 1986). A ^{6}LiH shield that absorbed effectively the neutrons scattered by the sample was added in the collimator of the spectrometer shield. The spectrometer was located 86.0 cm from the sample at an angle of 125 degrees with respect to the proton beam direction.   A simplified block diagram of electronic for the spectrometer is shown in Fig. 3. The pulse height signals of main detector were taken from the 12th dynode of photomultiplier, while the timing signals were taken from the anode. The stop signal for a TAC was taken from the time pick-off unit. The pulse height signals of Compton-suppression detectors were made by summing up the anode outputs from ten photomultipliers, and a discriminator level was set to 30 keV.

The high voltage for each of ten photomultipliers was adjusted so as to generate the same pulse height outputs for an ^{241}Am source at the center of detector.

2.3. Samples

Metallic foil samples were employed and the characteristics of samples are summarized in Table 1. The 15 mm diameter and 0.2 mm thick metal plate of ^{164}Dy is used for the capture cross-section measurement. A gold plate with a diameter of 15-mm and a thickness of 1.0 mm is used as a standard. Each capture sample was located at an angle of 0 degree with respect to the proton beam direction. The distance between the neutron source and the sample was 12 cm.

2.4. Data Taking

The runs with and without the sample (sample run and blank run) and the run with the standard gold sample (gold run) were made cyclically in each measurement to average out changes in experimental conditions such as the incident neutron spectrum. Since the measurements were carried out cyclically, systematic changes in experimental conditions could be corrected for. The blank run was performed in order to determine the background, and also to monitor any changes in the incident neutron energy and the thickness of the ^{7}Li neutron-target. The three runs were connected according to the neutron counts of the ^{6}Li-glass detector. Total running times were about 168 hours: 131.5, 19.5 and 17 hours for the sample, gold and blank runs, respectively.

3. DATA ANALYSIS

3.1 . Incident Neutron Spectra

The TOF spectrum observed with the ^{6}Li-glass detector for the blank runs is shown in Fig. 4. The TOF decreases with increasing channel number, because the reference pulses from the time pick-off unit were used as the stop signals of TAC. The sharp peak around 820 channel is due to the γ rays from the ^{7}Li(p, γ)^{8}Be reaction in the lithium target. The broad bump below 600 channel is due to the neutrons with energies less than 90 keV. Since the distance between the lithium target and the neutron detector was 30 cm, the TOF of the γ rays was 1.0 ns. Therefore, the TOF of the neutrons counted in the I-th channel, $T(I)$ (ns), was calculated as follows:

$$T(I) = T_{cal}(I_{\gamma} - I) + 1.0 \qquad (1)$$

where I_γ is the channel number of the γ-ray peak, and T_{cal} the channel width which was calibrated with a time calibrator. Then, the neutron energy in the laboratory system, E_n(MeV), was obtained by

$$E_n = \left(\frac{72.3 L}{T} \right)^2 ,$$

(2)

where T(ns) is the TOF of neutron and L(m) the flight path length. After subtracting a constant background, estimated from the counts around 700 channel, from the raw TOF spectrum, the net TOF spectrum, $n(T)$, was converted to the neutron energy spectrum, $n(E_n)$ using Eq. (2) and the detection efficiency, $\varepsilon(E_n)$, of the neutron detector.

$$n(E_n) = \frac{1}{\varepsilon(E_n)} n\left(\frac{72.3L}{\sqrt{E_n}} \right) \frac{72.3L}{2E_n \sqrt{E_n}}$$

(3)

The incident neutron energy spectrum is shown by solid circles (●) in Fig. 5, together with the transmitted neutron spectra for the sample (∇) and gold (■) runs. A cut-off energy was set to 10 keV for the $n(E_n)$, because the signal-to-noise ratios of TOF spectrum were not so good below 10 keV. The $n(E_n)$ has the maximum value around 30 keV.

3.2. Capture γ-ray Pulse Height Spectra

The observed TOF spectra with the γ-ray spectrometer for the (a) sample, (b) gold, and (c) blank runs are shown in Fig. 6. The sharp and intense peak around 630 channel is due to the γ rays from the ^{7}Li(p, γ)^{8}Be reaction, and the bump around 500 channel is due to the neutron capture γ rays from the ^{164}Dy or ^{197}Au sample. The (p, γ) peak width is about 4ns (FWHM) which is a measure of the total time resolution of the γ-ray detection system and the pulsed proton beam from the Pelletron accelerator. The neutron energy resolutions estimated for the neutron capture γ-ray bump using the time resolution of 4 ns and Eq. (2) with L=0.12 m were 14 keV at 60 keV, 5.0 keV at 30 keV and 2.7 keV at 20 keV.

Digital gates (DGs) were set in the foreground (FG) and background (BG) regions of the TOF spectra measured for the sample, gold, and blank runs, as shown in Fig. 6, to obtain FG and BG pulse height (PH) spectra. The BG level around 200 channel is identical to that around 900 channel within the statistical error and the BG level in Fig. 6(c) is constant over the whole region except for the (p, γ) peak. Thus, the net capture γ-ray PH spectra, $S(I)$, were obtained by subtracting the BG PH spectrum normalized with the ratio of gate widths from the FG PH spectra. The net capture γ-ray PH spectra for

(a) ^{164}Dy and (b) ^{197}Au in the incident neutron energy region of 15 to 90 keV are shown in Fig. 7.

3.3 Capture Cross Section

An average capture cross-section, $<\sigma>_k$, of ^{164}Dy or ^{197}Au for the k-th DG in the region of 10 to 90 keV was defined

$$<\sigma>_k = \frac{\int_{E_{k,min}}^{E_{k,max}} \sigma(E_n)n(E_n)dE_n}{\int_{E_{k,min}}^{E_{k,max}} n(E_n)dE_n},$$

(4)

$$Y_k = C_k \int_{E_{k,min}}^{E_{k,max}} N\sigma(E_n)\phi n(E_n)dE_n$$

$$= C_k N \left\{ \phi \int_{E_{k,min}}^{E_{k,max}} n(E_n)dE_n \right\} <\sigma>_k,$$

(5)

where $\sigma(E_n)$ is the capture cross section, and $E_{k,min}$ and $E_{k,max}$ are the low- and high-energy boundaries of the k-th DG, respectively. Then, the capture yield, Y_k, for the k-th DG was expressed as follows:

where N is the number of target nuclei per cm^2, ϕ the number of incident neutrons above the cut-off energy, and C_k the correction factor related to neutrons described below. The capture yield also can be described in terms of capture γ-ray PH spectrum, $S(I)$, and the weighting function of the γ-ray spectrometer, $W(I)$, as follows:

$$Y_k = \frac{\sum_I W(I)S_k(I)}{B_n + E'_{n,k}}$$

(6)

where B_n is the neutron binding energy of target nucleus and $E'_{n,k}$ the average incident neutron energy for the k-th DG in the center of mass system. The weighting function used for this analysis was the same one as the previous experiment (Mizuno *et al*. 1999):

$$W(I) = 2.415 \times 10^2 \sqrt{I} + 3.008I + 2.443 \times 10^{-1} I^2 - 2.955 \times 10^{-4} I^3$$

(7)

The average capture cross section, $<\sigma>_{k,Au}$, of ^{197}Au for the k-th DG was calculated from Eq. (4) with the evaluated values of ^{197}Au in ENDF/B-VI (Young 1984). Then, the number of incident neutrons for the k-th DG was obtained as follows:

$$\phi_k = \frac{Y_{k,Au}}{\left\{ C_{k,Au} N_{Au} <\sigma>_{k,Au} \right\}},$$

where N_{Au} is the number of Au nuclei per cm^2 and $C_{k,Au}$ the correction factor for the Au sample.

Finally, the average capture cross-section for ^{164}Dy was obtained as follows:

$$<\sigma>_{k,Dy} = \frac{M_{Au}}{M_{Dy}} \bullet \frac{N_{Au}}{N_{Dy}} \bullet \frac{C_{k,Au}}{C_{k,Dy}} \bullet \frac{B_{n,Au} + E_{n,k}^{'Au}}{B_{n,Dy} + E_{n,k}^{'Dy}} \bullet \frac{\sum_I W(I)S_{k,Dy}(I)}{\sum_I W(I)S_{k,Au}(I)} <\sigma>_{k,Au} \quad, \tag{9}$$

where M_{Au} and M_{Dy} are the neutron counts of the ^{6}Li-glass detector for the Au and Dy runs, respectively. The values of M_{Au} and M_{Dy} were corrected for the attenuation by the Au and Dy samples, respectively, because the Au or Dy sample existed between the neutron source and the neutron detector. Correction factors were evaluated considering the effects from the neutron self-shielding and the multiple-scattering, and the γ-ray scattering and absorption in the sample, from the dependence of the γ-ray detection efficiency on the γ-ray source position, from the impurities in the sample, and from the dead time. The overall correction factors obtained are less than 1.02 for Dy and 1.12 for Au.

5. RESULT AND DISCUSSION

The capture cross-sections of ^{164}Dy were measured in the neutron energy region of 10 to 90 keV. The total error is about 12%. In addition to the statistical error (10%), the following errors were taken into account for the capture cross-section measurements: the errors of the number of target nuclei (<1%), standard capture cross-sections of ^{197}Au (3%), weighting function of γ-ray spectrometer (4-6%), extrapolation of net capture γ-ray PH spectrum below the discrimination level (0.6 MeV) in deriving the capture yield with the PH weighting technique (2%), and corrections described above (1-2%). The present results are shown in Table 2 and in Fig. 8 compared with the previous measurements (Fawcett *et al*. 1972, Bokhovko *et al*. 1988, Voss *et al.* 1999) and the evaluation of ENDF/B-VI (Leonard *et al*. 1967). Very recently, Voss et al. (Voss *et al*. 1999) measured the capture cross-sections of ^{161,162,163,164}Dy in the region of 3 to 225 keV with the Karlsruhe 4π BaF$_2$ detector. They used the ^{7}Li(p,n)^{7}Be neutron source with a ns-pulsed proton beam from the Karlsruhe 3 MV Van de Graaff , and also used the capture cross-sections of ^{197}Au for the neutron flux normalization. However, it should be remembered that the standard cross sections of ^{197}Au adopted by the Karlsruhe group are about 5% smaller than those of ENDF/B-VI which were adopted by the present study. Therefore, if the standard values of ENDF/B-VI are used in their data analysis, their results become close to the present ones. The other difference is in the Dy samples, i.e., metal plate and oxide powder. Oxide powder is generally hygroscopic, and the effect of the water in the sample on the cross-section

measurement has to be taken into account in the analysis of experimental data. The reported errors for the cross-section ratios of Dy isotopes to ^{197}Au are about 1 –2 %. The present results are in good agreement with both the previous measurements done by Voss *et al*. (Voss *et al.* 1999) and Bokhovko *et al*. (Bokhovko *et al*. 1988), where they used oxide powder instead of a metal plate, and the evaluated values in the ENDF/B-V. However, the data measured by Fawcett *et al.* (Fawcett *et al*. 1972) were higher than any other results.

6. CONCLUSION

   The capture cross-sections of ^{164}Dy were measured with errors of about 12% in the incident neutron energy region of 10 to 90 keV, using a 1.5-ns pulsed neutron source by the ^{7}Li(p,n)^{7}Be reaction and an anti-Compton NaI(Tl) γ-ray spectrometer. The present results are in good agreement with both the previous measurements done by Voss *et al*. and Bokhovko *et al*., where they used dysprosium oxide powder instead of metal plate, and the evaluated values from the ENDF/B-VI.

REFERENCES

Bokhovko M. V., Kazakov L. E., Kononov V. N., Poletaev E. D., Timokhov V. M., Yad. Kons. **4** (1988) 8.

Booth R., Ball W. P., and MacGregor M. H., Phys. Rev. **112** (1958) 226.

Fawcett L. R., Furr A. K., Lindsay J. G., Nucl. Sci. and Eng. **49** (1972) 317.

Igashira M., Kitazawa H., Yamamuro M., Nucl. Instrum. Meth. **A245** (1986) 432.

Igashira M., Tanaka M., Masuda K., Proc. the 8th Int. Symp. On Capture Gamma-ray Spectroscopy and Related Topics (Fribourg, Switzerland, 1993), p.992 (1994).

Komano H., Ph. D. Thesis, Tokyo Institute of Technology, (1984).

Leonard B. R., Jr. and Stewart K. B. evaluation data from ENDF/B-VI data file for ^{164}Dy (MAT=6649), (1967).

Mizuno S., Igashira M., and Masuda K., J. Nucl. Sci. and Tech. **36** (1999) 493.

Shimizu M., Ph. D. Thesis, Tokyo Institute of Technology, (1985).

Voss F., Wisshak K., Arlandini C., and Kappeler F., Phys. Rev. **C59** (1999) 1154.

Young P. G. evaluation data from ENDF/B-VI data file (revised version 1) for ^{197}Au (MAT=7925), (1991).

Table 1. Characteristics of samples

Sample	^{164}Dy	^{197}Au
Weight (g)	0.3268	3.4274
Chemical purity (%)	98.45	99.99
Isotopic composition(%)		
^{197}Au	-	100
^{156}Dy	<0. 01	
^{158}Dy	<1. 01	
^{160}Dy	0.02	
^{161}Dy	0.15	
^{162}Dy	0.35	
^{163}Dy	1.03	
^{164}Dy	98.45	
Thickness (mm)	0.2	1.0
Diameter (mm)	15.0	15.0

Table 2. Measured neutron capture cross section of ^{164}Dy compared with the results of Voss *et al*. 1999

Average neutron energy [Energy Bin] (keV)	Present measurement (barn)	Voss et al. 1999 (barn)
18 [15-20]	0.328 ± 0.047	0.296
23 [20-25]	0.249 ± 0.033	0.235
28 [25-30]	0.277 ± 0.024	0.237
35 [30-40]	0.213 ± 0.012	0.198
45 [40-50]	0.186 ± 0.011	0.183
55 [50-60]	0.185 ± 0.011	0.164
69 [60-80]	0.162 ± 0.008	0.145

Fig. 1. Typical experimental arrangement

3MV-Pelletron accelerator

Anti-Compton NaI(Tl) Spectrometer

Pulsed Proton Beam
(1.5ns width, 2MHz or 4MHz)

^{7}Li-target

Sample

125°

2.38°

^{6}Li-glass Scintillation
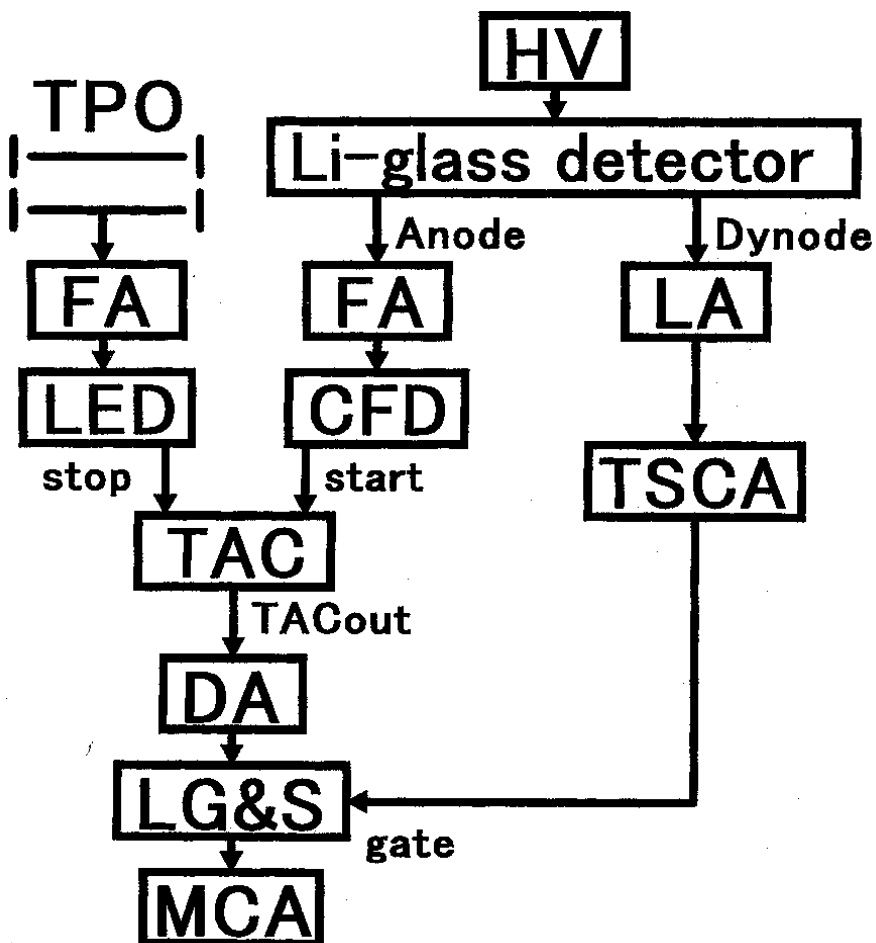
NaI(Tl)

Borated Paraffin or
Borated Polyethylene

Pb

^{6}LiH

Cd
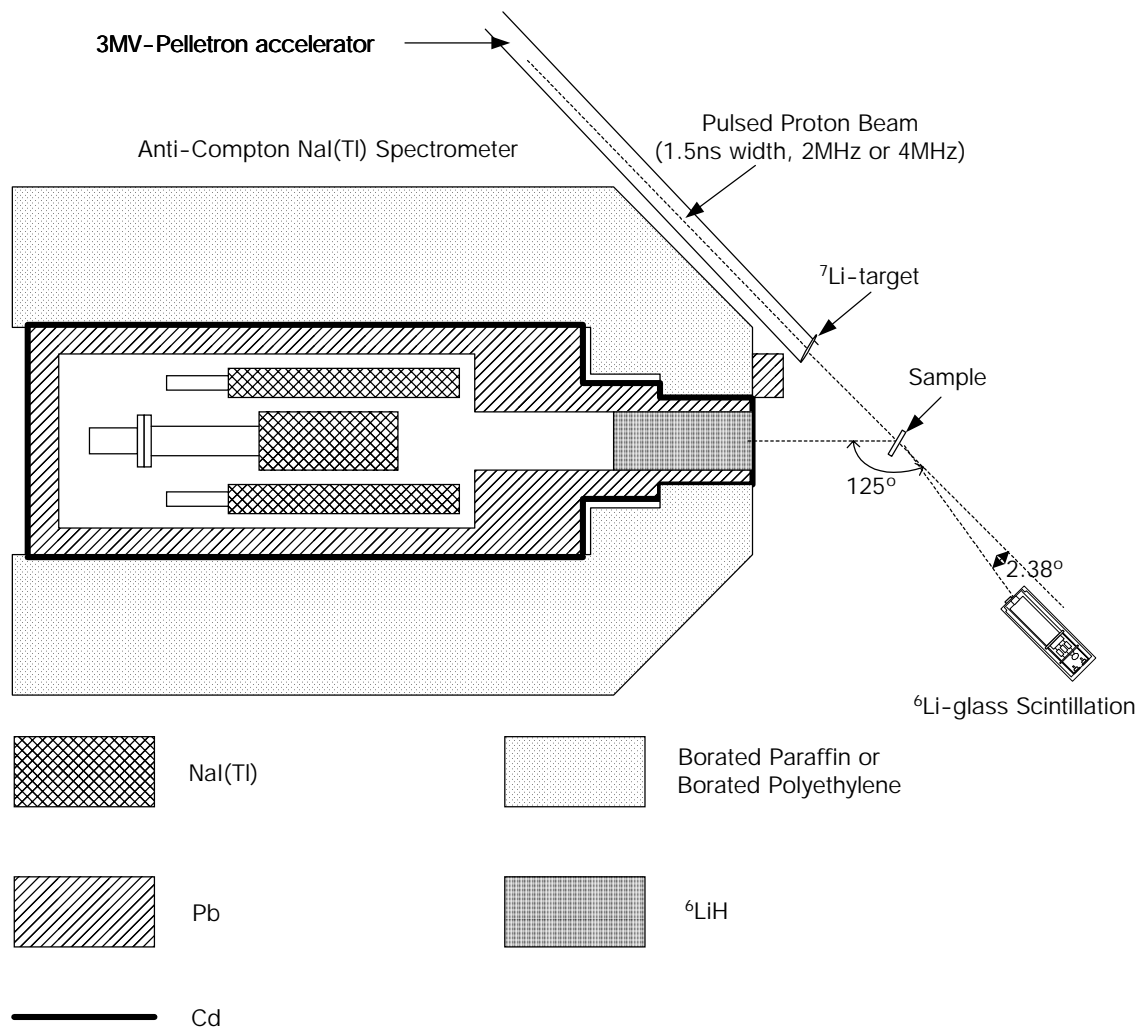
Fig. 2. A block diagram of electronics for the ^{6}Li-glass detector

CFD Constant Fraction Discriminator
DA Delay Amplifier
FA Fast Amplifier
HV High Voltage
LA Linear Amplifier
LED Leading Edge Discriminator
LG&S Linear Gate and Stretcher
MCA Multi-Channel Analyzer
TAC Time to Amplitude Converter
TPO Time Pick-Off Unit
TSCA Timing Single Channel Analyzer

Fig. 3. A block diagram of electronics for the anti-Compton NaI(Tl) spectrometer
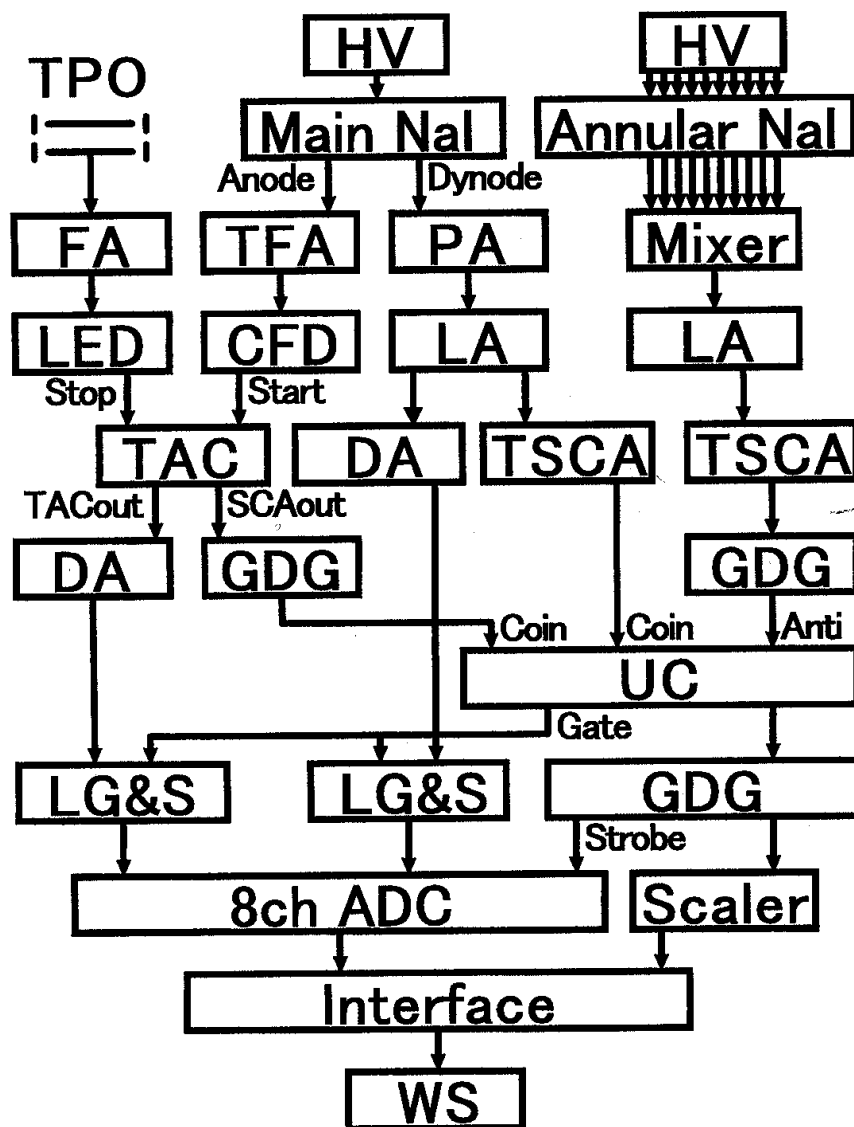
HV : High Voltage
TPO : Time Pick-Off Unit
FA : Fast Amplifier
PA : Pre Amplifier
LA : Linear Amplifier
DA : Delay Amplifier
UC : Universal Coincidence
WS : Work Station

TFA : Timing Filter Amplifier
LED : Leading Edge Discriminator
CFD : Constant Fraction Discriminator
TAC : Time to Amplitude Converter
TSCA : Timing Single Channel Analyzer
GDG : Gate and Delay Generator
LG&S : Linear Gate and Stretcher
ADC : Analog to Digital Converter

Fig. 4. Typical TOF spectra observed with the ^{6}Li-glass detectors for the blank runs
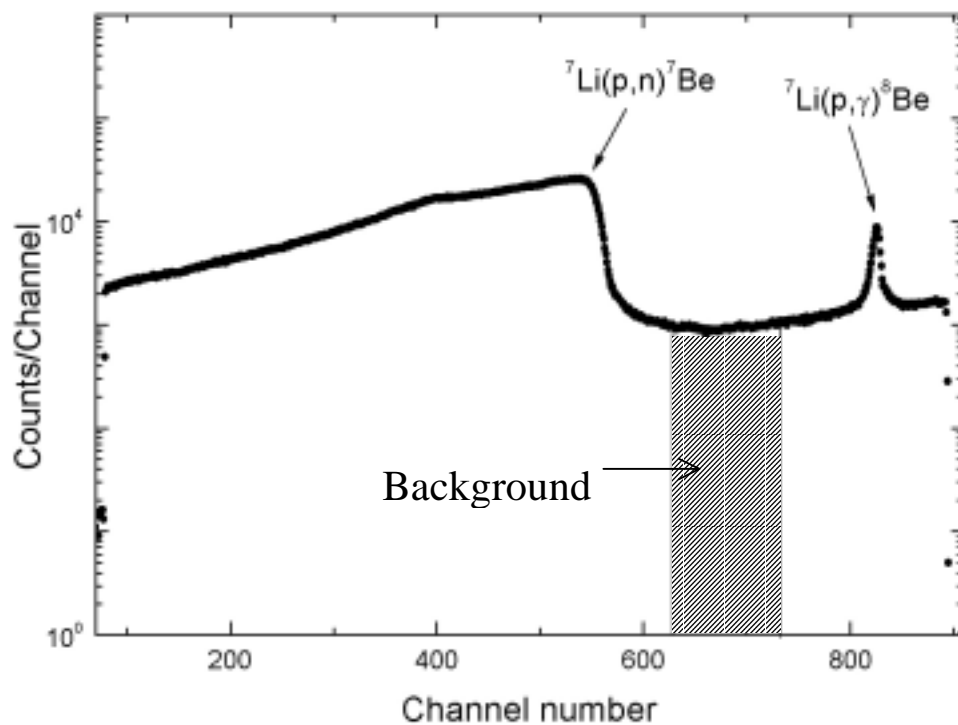
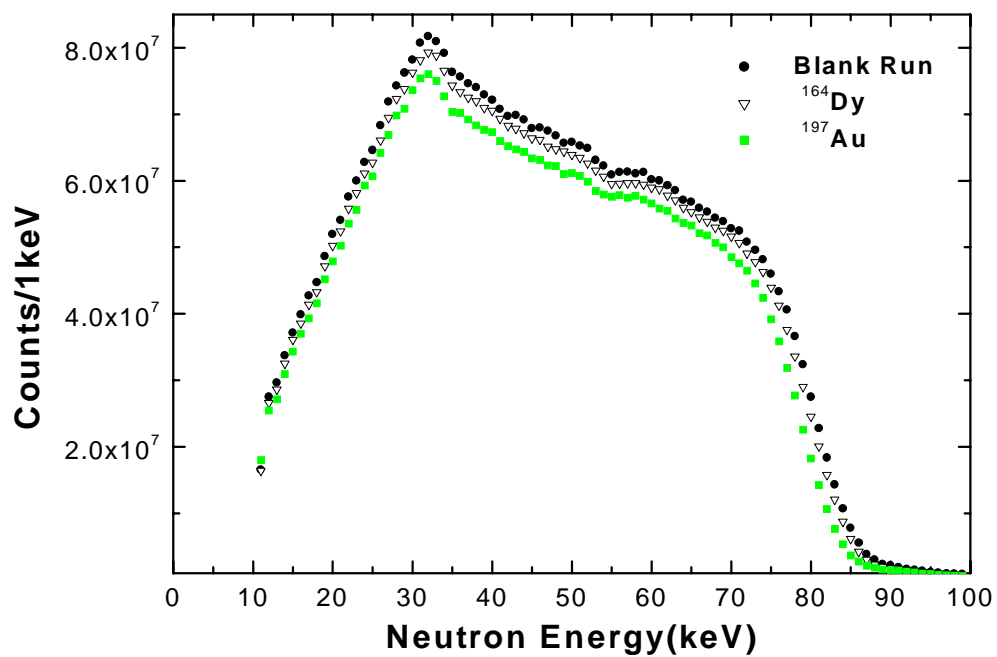Fig. 5. Incident neutron energy spectrum (●) and the transmitted neutron spectra for the sample (∇) and gold (■) runs

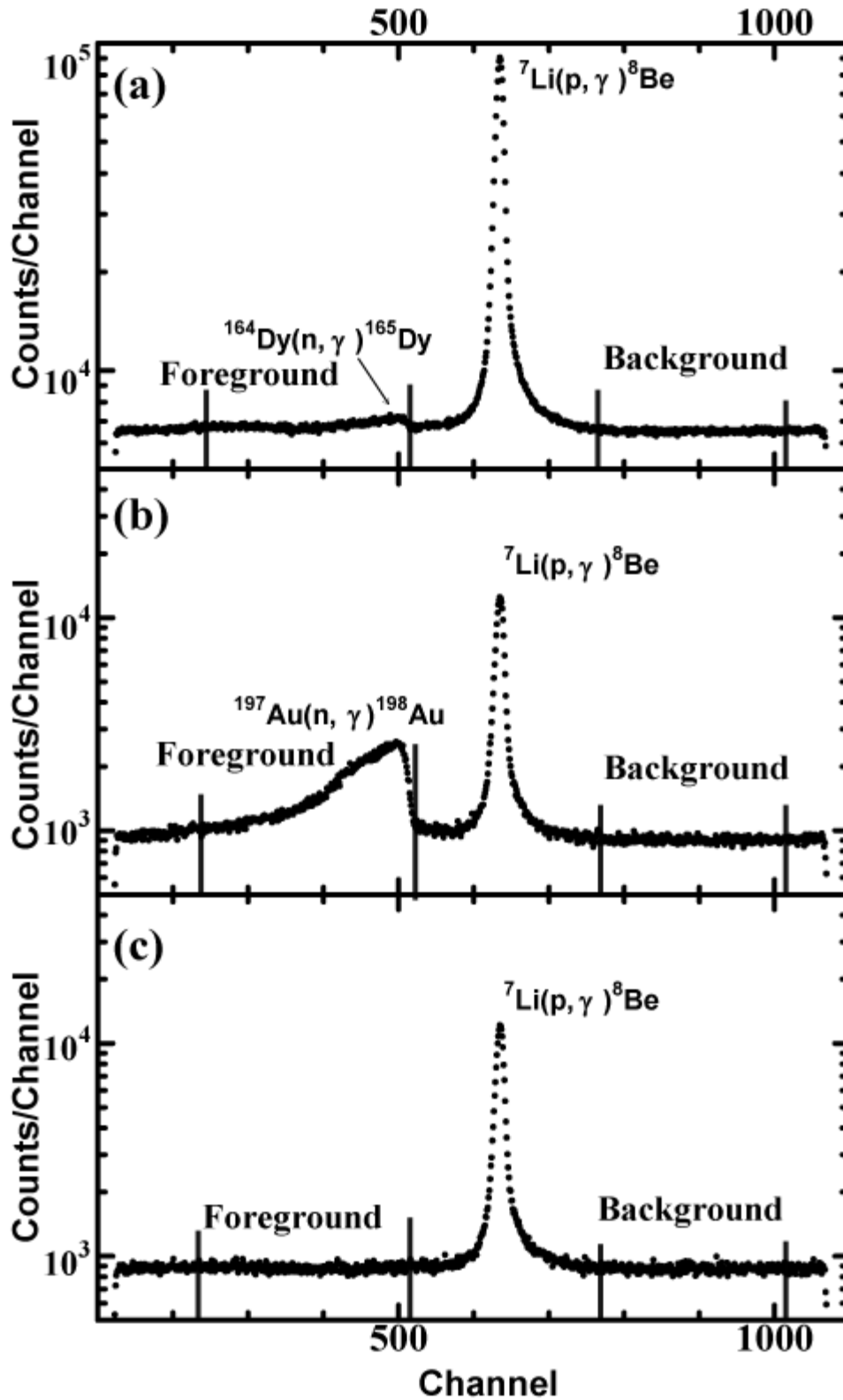Fig. 6. TOF spectra observed with γ-ray spectrometer for (a) [164]Dy, (b) [197]Au, and (c) blank run

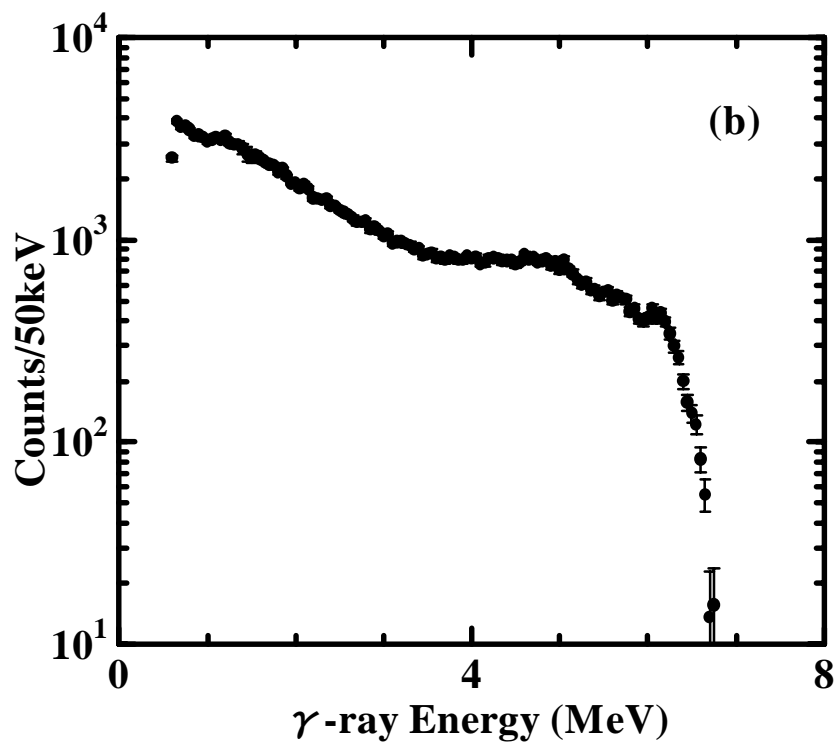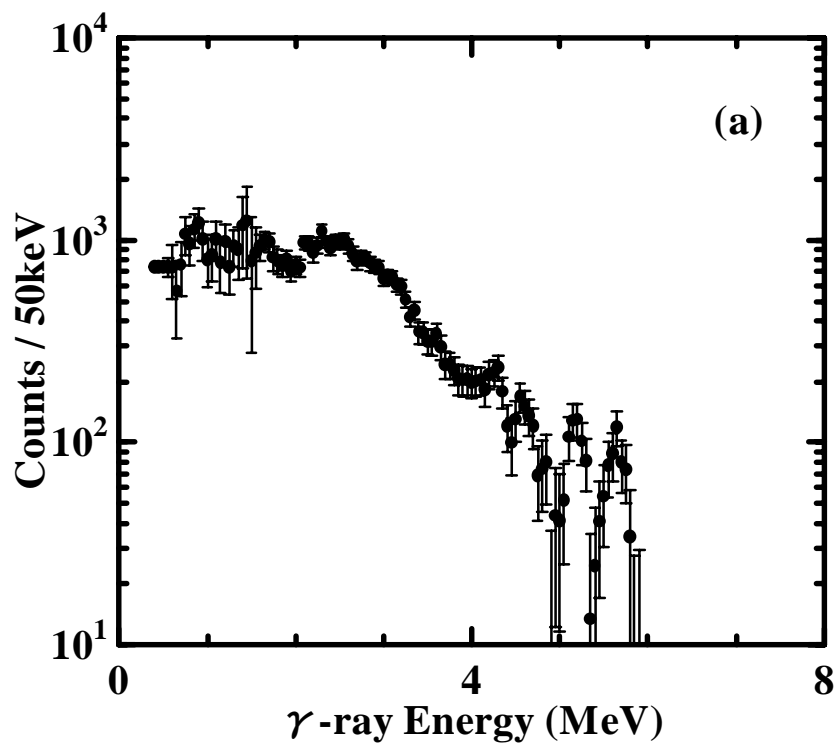Fig. 7. Observed capture γ-ray PH spectra of (a) [164]Dy and (b) [197]Au

Fig. 8. Neutron capture cross sections of ^{164}Dy in the keV region